RESEARCH ARTICLE

Going underground: soil hydraulic properties impacting maize responsiveness to water deficit

Tina Koehler [ORCID] · **Daniel Sebastian Moser** · **Ákos Botezatu** · **Tharanya Murugesan** · **Sivasakthi Kaliamoorthy** · **Mohsen Zarebanadkouki** · **Manuela Désirée Bienert** · **Gerd Patrick Bienert** · **Andrea Carminati** · **Jana Kholová** · **Mutez Ahmed**

Abstract

Purpose Although the coordination between stomatal closure and aboveground hydraulics has extensively been studied, our understanding of the impact of belowground hydraulics on stomatal regulation remains incomplete. Here, we investigated whether and how the water use of maize (*Zea mays* L.) varied under hydraulically contrasting soil textures. Our hypothesis is that a textural-specific drop in the hydraulic conductivity is associated with a distinct decrease in transpiration during soil drying.

Responsible Editor: Doris Vetterlein.

T. Koehler (✉) · A. Carminati
Physics of Soils and Terrestrial Ecosystems, Department of Environmental Systems Science, ETH Zürich, Zurich, Switzerland
e-mail: tina.koehler@usys.ethz.ch

T. Koehler · D. S. Moser · Á. Botezatu ·
M. Zarebanadkouki · M. Ahmed
Soil Physics, Bayreuth Center of Ecology and Environmental Research (BayCEER), University of Bayreuth, Bayreuth, Germany

T. Murugesan · S. Kaliamoorthy · J. Kholová
Crop Physiology, International Crops Research Institute for Semi-Arid Tropics, Patancheru, India

Methods Maize plants were grown in contrasting soil textures (sand, sandy loam, loam) and exposed to soil drying. We measured the relationships between transpiration rate, soil water content as well as soil and leaf water potential. We used a soil-plant hydraulic model to reproduce the experimental observations and infer the hydraulic conductance of the soil-plant system during soil drying.

Results We observed the impact of soil texture on plant response to soil drying in various relationships. The soil water potentials at which transpiration decreased were more than one order of magnitude more negative in loam than in sand. The soil-plant conductance decreased not only abruptly but also at less negative soil water potentials in sand than in sandy loam or loam. Stomata closed at less negative leaf water potentials in sand than in loam. The

M. D. Bienert · G. P. Bienert
Crop Physiology, TUM School of Life Sciences, Technical University of Munich, Freising, Germany

J. Kholová
Information Technologies, Faculty of Economics and Management, Czech University of Life Sciences Prague, Prague, Czech Republic

M. Ahmed
Department of Land, Air and Water Resources, University of California Davis, Davis, CA, USA

model predictions matched well the experimental observations.

Conclusion The results elucidated that the critical soil water content and potential at which plants close stomata depends on the soil texture. These findings support our plea to include soil properties for understanding and predicting stomatal regulation during soil drying.

Introduction

Plant water deficit occurs when the availability of soil water cannot match plant water demand for growth and transpiration (Draye et al. 2010; Tardieu et al. 2018). Water flow across the soil-plant-atmosphere continuum (SPAC) is driven by transpiration, which creates a suction within the xylem. The suction drives the water flow from the soil to the roots along a gradient of potentials within the SPAC. The flow is proportional to the differences in water potentials and the hydraulic conductance of the components of the SPAC. The transpiration rate is set by atmospheric conditions and, on a short timescale, is regulated by stomatal opening and closing (Ahmed et al. 2018a; Brodribb et al. 2019; Buckley 2019). Plants are capable of altering the hydraulic conductivity of their compartments to adapt to changing environmental conditions. Examples for that would be the adaptation of root hydraulic conductance by differential aquaporin expression, or stomatal conductance regulation in response to abscisic acid (ABA), a key hormone involved in plant response to water stress, and their interaction (Rodrigues et al. 2017). Moreover, plant growth adaptation to different edaphic conditions might change the hydraulics of above- as well as belowground compartments (Lynch 2019; Parent et al. 2009). However, our mechanistic understanding of this hydraulic acclimatization is rather incomplete.

Although more than 80% of terrestrial evapotranspiration passing through stomata and transpiration represents by far the largest water flux globally (Jasechko et al. 2013), we still lack a consensus on what triggers stomatal closure during soil drying. It was shown that stomata functioning is regulated by two main mechanisms: a passive mechanism induced by the hydraulic connection between epidermal and guard cells (Buckley 2019), and an active mechanism, the production of hormones, such as ABA (Brodribb and McAdam 2017). How soil drying impacts stomatal conductance has yet to be revealed and incorporated in existing models of stomatal response to drought in order to potentially improve their performance (Anderegg et al. 2017).

In wet soil, it is generally believed that the plant hydraulic conductance is setting the limits to water flow (Hopmans and Bristow 2002; Passioura 1980). Under dry soil conditions, however, a texture-specific loss of soil hydraulic conductivity of more than 10 orders of magnitude occurs (Draye et al. 2010), limiting the water supply to the leaves. This is due to an enhanced water depletion in close proximity to the roots and a relatively high water flux near the roots (caused by the radial water flow into the roots), thus, leading to a large drop in matric water potential closer to the roots (Abdalla et al. 2021, 2022; Gardner 1960). Carminati and Javaux (2020) hypothesized that this drop in matric potential is the primary driver of stomatal closure and supported this hypothesis by means of a meta-analysis and simulations. This hypothesis has been investigated in tomato (*Solanum lycopersicon* L.) (Abdalla et al. 2021) and maize (*Zea mays* L.) (Cai et al. 2021; Hayat et al. 2020). For instance, Cai et al. (2021) examined the response of maize (*Z. mays* L.), with and without root hairs, under two contrasting soil textures. The authors found that, in maize, soil texture rather than root hairs control water uptake and plant response to drought. Similarly, Rodriguez-Dominguez and Brodribb 2020 showed that, in olive trees, the loss of conductivity at the root-soil interface was the main driver of stomatal closure during soil drying.

In the light of these recent findings, the overall objective of this study is to emphasize the need of including soil and root traits in predicting transpiration behavior under soil drying (Atkinson et al. 2014). We measured the relationship between transpiration rate (E) and soil water content (θ), soil water potential (Ψ_{soil}) as well as leaf water potential (Ψ_{leaf}) of maize (*Z. mays* L.) grown in four soil textures and exposed to soil drying. We used a soil-plant hydraulic model to reproduce the experimental observations to be able to quantitatively describe the main biophysical processes of plant drought responsiveness as affected by

hydraulically differing soils. The soil-plant hydraulic model enabled us to infer the hydraulic conductance of the soil-plant system (K_{sp}, Carminati and Javaux 2020). Our hypothesis is that belowground hydraulic properties have a major impact on transpiration during soil drying. Specifically, we hypothesize that the drop in the soil hydraulic conductivity of the rhizosphere, the soil in the immediate vicinity of roots, is associated with the closure of stomata.

Material and methods

This study evaluates two experiments, carried out at two different locations. The first experiment was carried out at the International Crop Research Institute for the Semi-Arid Tropics in Patancheru (ICRISAT, Lat. 17.511100, Long. 78.275204), using two soils typical for the region. This experiment will be referred to as experiment 1 (exp. 1) in the following. The second part was conducted at the University of Bayreuth (Lat. 49.929858, Long. 11.579954), using another two soils. This experiment will be referred to as experiment 2 (exp. 2) in the following. The experimental procedure and tested genotypes were the same in both sets of experiments, allowing us to analyze the results of four different soil textures in total. In the following, the differences in growth conditions and the definition of the water stress levels are described separately, whereas the experimental procedure is explained universally for both experiments.

Plant material and growth

Experiment 1 We used maize (*Z. mays* L. root hairless mutant *rth3* and the corresponding wild-type B73) plants that were grown in glasshouse conditions under natural daylight oscillations and with day/night temperature averages of 31.2/25.7 °C and relative humidity of 79/67%. Plants were grown in pots (26.6-27.5 cm in diameter) filled with 8 kg of two different soils: sandy loam, and sand (which consisted of three parts sand to one part sandy loam). The soils were sieved to a particle size smaller than 1 cm to ensure homogeneous soil packing. Di-ammonium phosphate at a rate of 2.5-3 g per pot was applied before sowing. A data logger (Tinytag Ultra 2 TGU-4500 Gemini Datalogger Ltd., Chichester, UK) was positioned at plant canopy height to record glasshouse temperature and relative humidity (RH) % on a half-hourly basis. All pots were initially fertilized with 300 ml of nutrient solution [Macronutrients - $MgSO_4$(2.05 mM), K_2SO_4(1.25 mM), $CaCl_2.2H_2O$ (3.3 mM), KH_2PO_4 (0.5 mM), Fe-EDTA(0.04 mM), Urea(5 mM); and Micronutrients - H_3BO_3(4 μM), $MnSO_4$(6.6 μM), $ZnSO_4$(1.55 μM), $CuSO_4$(1.55 μM), $CoSO_4$(0.12 μM), Na_2MoO_4(0.12 μM)]. Additionally, pots filled with sand were fertilized a second time with two times 1 L of nutrient solution.

In total, there were four treatments: well-watered and three water stress levels, which differed in soil water content. Per water-stress level, only the most uniform plants (in terms of plant size in order to achieve similar stress levels in a given time) were considered for measurements, resulting in 5-7 replicates per water-stress level. In total, this resulted in 59 measured plants. The desired soil water contents of the water stress levels were reached by soil drying, meaning that when the targeted soil water content was reached, the related measurements were conducted (see below). The experimental design was completely random with the treatment as the first main factor, soil textures as the second main factor, and genotypes as subfactors.

Three water stress levels were determined from a dry down pre-experiment. Under comparable conditions like the here presented main experiment, the soil textural specific critical soil water content at which plants started decreasing transpiration in response to soil drying was determined for the used soils by a linear plateau regression (Supplementary Fig. 1). Thus, the soil water content of the water stress levels at which leaf water potentials were measured refer to: soil water content in well-watered conditions (WW), soil water content shortly before the previously determined decrease in transpiration (e.g. Kholová et al. 2010) in response to decreasing soil water content (WS1), soil water content around the decrease in transpiration (WS2) and soil water content shortly after the expected drop in transpiration (WS3).

Experiment 2 The same maize genotypes were grown in growth chamber conditions with a photoperiod set at 12 h/12 h and with day/night temperature averages of 22.6/18.8 °C and relative humidity of 67/68%. Plants were grown in columns (7 cm in diameter, 25 cm height) filled with 1.1 (loam)-1.3 (sand) kg of two different soil textures: a sand

substrate (mixture of 83.3% of quartz sand and 16.7% of loam) and loam (100% loam). The soils were sieved to a particle size smaller than 1 mm. A data logger (Easylog USB Data Logger (EL-USB-1), Lascar electronics, Wiltshire, UK) recording temperature and relative humidity (RH) % on a 10 min basis was positioned at plant canopy height. Fertilizer was applied in different amounts for both soils in order to supply the plants in the different substrates with the same amount of nutrients. The following nutrients were added per soil texture: sand: 100 mg (nutrient) kg^{-1} (soil) NH_4NO_3, 80 mg kg^{-1} $CaHPO_4$, 100 mg kg^{-1} K_2SO_4, 50 mg kg^{-1} $MgCl_2$ x $6H_2O$, 100 mg kg^{-1} $CaSO_4x2H_2O$, 3.25 mg kg^{-1} $MnSO_4$ x H_2O, 0.79 mg kg^{-1} $Zn(NO_3)_2$ x $4H_2O$, 0.5 mg kg^{-1} $CuSO_4 \times 5\ H_2O$, 0.17 mg kg^{-1} H_3BO_3, 3.25 mg kg^{-1} Fe-EDTA; loam: 50 mg kg^{-1} NH_4NO_3, 40 mg kg^{-1} $CaHPO_4$, 50 mg kg^{-1} K_2SO_4, 25 mg kg^{-1} $MgCl_2$ x $6H_2O$.

In total, there were four treatments; well-watered and three water stress levels. Per water-stress level, only the most uniform plants (in terms of plant size in order to achieve similar stress levels in a given time) were considered for measurements, resulting in 2-6 replicates per water-stress level. In total, this resulted in 40 measured plants.

The water stress levels were determined from the decrease in transpiration. Plants were defined to be in well-watered conditions (WW) when their normalized transpiration ratio (NTR, see definition of NTR in 2.3) was at one, meaning they transpired maximally, whereas the water stress levels were defined by a decrease in transpiration by: 20-30% (NTR 0.8-0.7) for WS1, by 40-50% (NTR 0.6-0.5) for WS2 and by more than 70% (NTR < 0.3) for WS3.

The contrasting genotypes were initially chosen in order to reveal the effect of root hairs in maize under soil drying. However, no genotype-specific differences were found on a behavioral level (transpiration response to soil drying) as well as on a molecular level (leaf ABA in water stressed conditions). Therefore, we counted them as replicates for the same sample (Supplementary note S1).

Soil hydraulic properties

The soils were characterized by measuring their hydraulic properties using HYPROP2 (METER EVIRONMENT, München, Germany). The water retention was fitted using the bimodal porosity model of van Genuchten (Durner 1994):

$$\frac{\theta(h) - \theta_r}{\theta_s - \theta_r} = \sum_{i=1}^{k} w_i \left[\frac{1}{1 + (\alpha_i|h|)^{n_i}} \right]^{m_i}, \qquad (1)$$

with $|h|$ (cm) being the absolute soil water potential, θ_r and θ_s being the residual and saturated soil water content (cm^3/cm^3), respectively, k referring to the number of subcurves considered (k=2), w_i being the weighing factors between the subcurves, α_i (cm^{-1}) representing the air entry capillary pressure inversely for a subcurve, and n_i and m_i being empircal parameters for the subcurves (m_i=1-1/n_i). The fitted parameters can be found in Supplementary Table 1.

Further information regarding soil physical and chemical properties can be found in Pathak et al. (2013) for experiment 1 and in Vetterlein et al. (2021) for experiment 2.

Transpiration and leaf water potential measurements

The soil was saturated and allowed to drain overnight. Additionally, a layer of plastic beads was applied on the soil surface to minimize direct evaporation from the soil. In the following, the plants determined to be measured in well-watered conditions remained constantly watered up to around 80% field capacity, while the remaining plants were exposed to water stress by partially compensating for water loss from transpiration to prevent too rapid dehydration (Gahoonia and Nielsen 2003). Pots were subsequently weighed every morning. Daily transpiration was calculated as the difference in weight of each pot on successive days plus the water added to the pot between two successive weighing (Devi et al. 2010). Transpiration values were normalized in two-steps to facilitate comparison. First, a transpiration ratio (TR_i [mg]) for each plant of each day was calculated by dividing the transpiration of each drying pot (T_{dry} [mg]) by the average transpiration rate of the control pots in well-watered conditions (T_{WW} [mg]) to account for variabilities in transpiration rate among plants of the same genotype as (Kholová et al. 2010):

$$TR_i = \frac{T_{dry}}{T_{WW}} \qquad (2)$$

In a second step, TR_i was normalized to get the normalized transpiration ratio (NTR_i) for each pot to account for plant growth over time. This was done by calculating the initial average transpiration ratio for each pot (TR_{av} [mg]]) over the first four days after cessation of irrigation, when the plants were still in well-watered conditions. Daily TR_i was divided by TR_{av} as (Devi et al. 2010):

$$NTR_i = \frac{TR_i}{TR_{av}} \qquad (3)$$

Values of soil water content were measured by a time-domain reflectometer (TDR, E-Test, Lublin, Poland, rod length: 10 cm) on days of leaf water potential measurements by inserting the TDR vertically in the pot on the respective days. Leaf water potentials were measured on the day when the desired soil water content/ decrease in transpiration was reached in the course of soil drying. Soil matric potential (h [hPa]) was estimated from water content measurements by inverting the bimodal porosity model of van Genuchten (Durner 1994) towards the soil matric potential. Leaf water potential (Ψ_{leaf}) was determined at the 6th, 7th or 8th leaf stage (depending on availability) by day and under pre-dawn conditions (Ψ_{PD}) using the Scholander pressure chamber (Field plant water status console, UGT, Müncheberg, Germany). Under pre-dawn conditions, transpiration is assumed to be zero and water potential in roots and soil are expected to be in equilibrium (Ritchie and Hinckley 1975). Therefore, it serves as a proxy for soil water potential (Ψ_{soil}) as actually experienced by the plant.

The following morning, the procedure was repeated. Besides, transpiration was recorded every 1.5 – 2 hours between 08:30 and 13:00 throughout the experiment. The experiment was terminated when the leaf water potential was determined to be measured. The leaf water potential was measured once the desired soil water content of the water stress levels was reached in the soil drying process. Mean values and standard deviation of the measured parameters can be found in Supplementary Table 2. Subsequently, the leaf area of the whole plant was measured using the leaf area meter (LI-3100C AREA METER, LICOR, Bad Homburg, Germany), as well as the dry weight of the single parts (Supplementary Table 3). The time required to reach the predescribed stress

level after the last application of irrigation water took 22-27 (exp. 1) and 9-16 (exp. 2) days. By the end of the experiment, plants were 43-48 (exp. 1) and 37-47 (exp. 2) days old and still in vegetative stage.

Soil plant hydraulic model and assumptions

A soil-plant hydraulic model was used to simulate the relation between water potentials in soil, xylem and leaves and the transpiration rate. The water flow equations across soil and plants were solved for each compartment of the SPAC, as explained in detail in Carminati and Javaux (2020), Cai et al. (2020), and Hayat et al. (2020) and in Supplementary note S2 and supplementary Table 4.

The model assumes one single root to represent all roots active in water uptake. Root water uptake is taken to be uniform and described on the basis of a radial geometry. Soil water flow along a gradient in water potential from the soil to the leaves is calculated based on the premise that the hydraulic conductance of the components of the SPAC is proportional to the difference in water potentials.

To match the relationships between E and Ψ_{soil} as well as E and Ψ_{leaf}, we inversely modelled this relation by adjusting the plant hydraulic resistance (R_p) and by fitting the active root length (L). The plant hydraulic resistance is inversely related to its hydraulic conductance ($R_p=1/K_p$), which, in turn is equivalent to the soil-plant hydraulic conductance (K_{sp}) in well-watered conditions and given by the ratio between E and the difference between Ψ_{leaf} and Ψ_{soil}:

$$K_{sp} = \frac{E}{\Psi_{soil} - \Psi_{leaf}} \qquad (4)$$

In this case, Ψ_{soil} was taken to be indicated by Ψ_{PD}. Therefore, K_p was directly estimated from the the slope of the relationship between measured E and Ψ_{leaf} in well watererd conditions, while L was allowed to change to fit the named relationships. The confidence intervals of L have been determined by bootstrapping.

Simple hypothesis testing for goodness-of-predictions could not be performed as the data do not fulfill the requirements of the errors being independent, identically and normally distributed (Supplementary Fig. 2). Therefore, the goodness of fit was calculated according to Barnston (1992):

$$RMSE = \sqrt{\frac{\sum_{i=1}^{N}(\hat{y}_i - y_i)^2}{N}}, \qquad (5)$$

with N being the sample size, $\hat{y}$ being the predicted value based on the soil plant hydraulic model and y being the actual measurements of the dependent variable. In order to facilitate comparison between the goodness of simulations for different soils, $RMSE$ was normalized ($NRMSE$) by the range of the scale of the dependent variable, when they differed (e.g. when TR has not already been normalized to NTR).

At any soil water potential, there is a critical E at which the slope of the relationship between E and Ψ_{leaf} becomes nonlinear, depending on the hydraulic conductivities of the components of the SPAC. The onset of nonlinearity is defined as the point of stomata closure and hence downregulation of transpiration. The linear and nonlinear parts have been divided as follows: first, a slope (S_{leaf}) of iso-potentials is calculated for each soil water potential:

$$S_{leaf}(\Psi_{leaf}, \Psi_{soil}) = \left.\frac{\partial E}{\partial \Psi_{leaf}}\right|_{\Psi_{soil}}. \qquad (6)$$

Secondly, the relative decrease in S_{leaf} is calculated by the ratio between S_{leaf} and the maximal slope ($S_{leaf,\,max}(\Psi_{soil})$). The threshold beyond which the drop in leaf water potential was considered significant relative to a small increase in transpiration was set to 70% as:

$$\frac{S_{leaf}(\Psi_{leaf}, \Psi_{soil})}{S_{leaf,\max}(\Psi_{soil})} < 70\% \qquad (7)$$

The 70% was arbitrary but in a range of 70-90%, the suggested stomata closure shows little sensitivity to the chosen percentage (Carminati and Javaux 2020).

Sensitivity analysis

We conducted a sensitivity analysis of the value of the active root length (L) to the plant hydraulic resistance ($R_p = 1/K_p$) to evaluate the uniqueness of the solution. To get an appraisal of the confinement of L, the simulation of the E - Ψ_{leaf} relationship was generated using various possible values for R_p.

Results

Due to differences in growth conditions between plants in the two sets of experiments, exp. 1 sandy loam and exp. 1 sand were compared to each other separately from the soils that have been tested in experiment 2.

In experiment 1, sandy loam had the highest gravimetric water (θ) content at any given matric potential (Fig. 1A). Water content in sandy loam decreased rather continuously, while the sand (exp. 1) showed a relatively steep decrease in water content over a small range of water potential (Fig. 1A). The two soils have similar hydraulic conductivity curves (Fig. 1B). However, considering both scales being logarithmic, even seemingly small differences express deviations of up to one order of magnitude. In sand (exp. 1), soil hydraulic conductivity (K_s) decreased at almost 3 fold higher (= less negative) Ψ_{soil} (−0.0011 MPa) than in sandy loam (−0.0028 MPa) at a slightly higher rater (sand (exp. 1): −1.8679*10^{-08}, sandy loam: −7.3363*10^{-09}). For the soils tested in experiment 2, sand (exp. 2) exhibits a much steeper water potential gradient with a lower water retention in general, compared to the loam (Fig. 1C). The soil hydraulic conductivities vary considerably. The sand (exp. 2) shows a 2.6 times higher saturated conductivity. K_s decreased at slightly less negative Ψ_{soil} in loam (−0.0021 MPa) than in sand (exp. 2, −0.0025 MPa), but the sand (exp. 2) exhibits a much steep decrease in hydraulic conductivity over a relatively small range of matric potentials (sand (exp. 2): −8.3194*10^{-07}, loam: −8.0438*10^{-08}, Fig. 1D) which is linked to the drainage of most soil pores in this range of potentials (Fig. 1C).

We observed a clear difference between the soil textures in their NTR response to declining θ in both experiments. In experiment 1, the output of the soil plant hydraulic model suggests a decrease in NTR at the highest water content in sandy loam (18 vol.-%), followed by sand (exp. 1, 11 vol.-%, Fig. 2A) . The confidence intervals of the observations and the predictions do not overlap between the two soil textures, indicating a pronounced difference between sandy loam and sand (exp. 1). In experiment 2, NTR drops at higher θ in loam (13 vol.-%) than in sand (exp. 2, 11 vol.-%, Fig. 2B). The confidence intervals of the measurements largely overlap, suggesting no significant difference between soil textures (Fig. 2B).
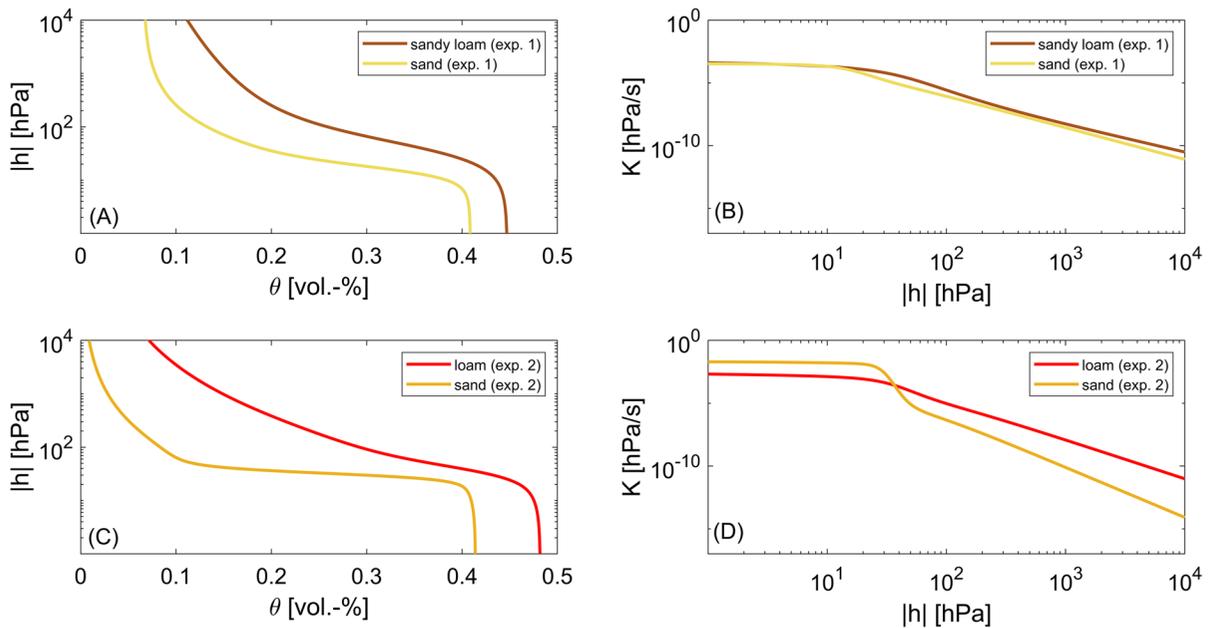
Fig. 1 Soil hydraulic properties of the examined soil textures: **(A)** water retention- and **(B)** soil hydraulic conductivity curves for exp. 1 sandy loam and sand, **(C)** water retention- and **(D)** soil hydraulic conductivity curves for exp. 2 loam and sand
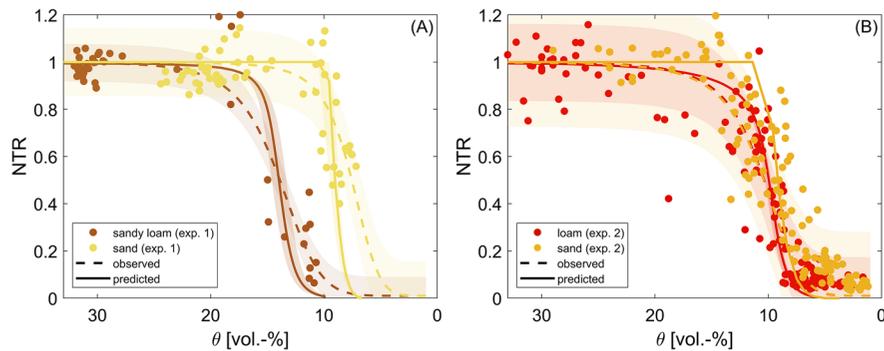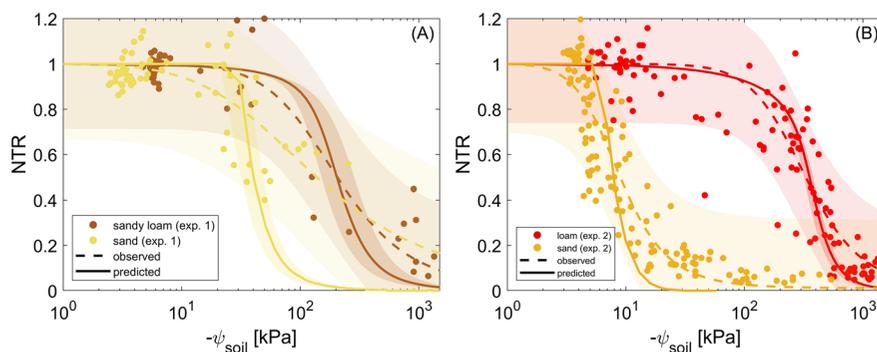

Fig. 2 Normalized transpiration ratio (*NTR*) response to decreasing soil water content (θ) between different soil textures as mean values of the measurements (dots), the empirical fit of the observations (dashed line with confidence intervals) and as predcited by the soil-plant hydrauic model (solid line with confidence intervals) for: **(A)** exp. 1 sandy loam and sand, and for **(B)** exp. 2 loam and sand

In both experiments, the data were well reproduced by the model as indicated by a relatively low RMSE (Supplementary Table 5).

Also in the relationship between *NTR* and Ψ_{soil}, pronounced differences between the soil textures become visible with soil drying. *NTR* decreases at higher Ψ_{soil} in sand (exp. 1, −0.0158 MPa) compared to sandy loam (−0.0370 MPa, Fig. 3A) in experiment 1. This trend is pronounced in the simulations

as indicated by non-overlapping confidence intervals. However, the overlapping confidence intervals of the observations suggest this difference not to be significant (Fig. 3A). In experiment 2, *NTR* drops at a more than one order of magnitude higher Ψ_{soil} in sand (exp. 2, −0.0052 MPa), compared to in loam (−0.1239 MPa, Fig. 3B). This becomes clear in the predictions as well as in the observations. The confidence intervals of the measurements as well as of

Fig. 3 Normalized transpiration ratio (*NTR*) response to decrease in soil water potential (Ψ_{soil}) between different soil textures as mean values of the measurements (dots), the empirical fit of the observations (dashed line with confidence inter-
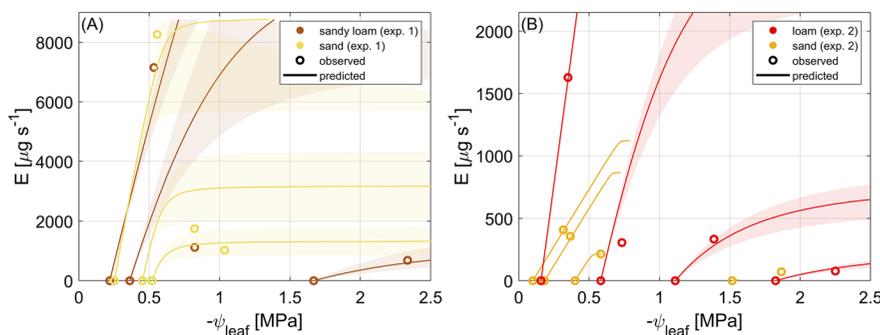
vals) and as predcted by the soil-plant hydrauic model (solid line with confidence intervals) for: **(A)** exp. 1 sandy loam and sand, and for **(B)** exp. 2 loam and sand

the predictions do not overlap, suggesting plants to respond significantly different to the varying soil textures (Fig. 3B). In both sets of soils, the model reproduced the experimental observation well as indicated by a relatively low RMSE (Supplementary Table 6) and the model simulation lying within the confidence intervals of the observed data (Fig. 3).

We used the conceptual and numerical modelling framework to reproduce the relation between mean transpiration rate and leaf water potential (Supplementary Table 4) at different levels of soil water potential. Subsequently, we inferred the soil-plant hydraulic conductivity (K_{sp}, as shown by the slope of the $E - \Psi_{leaf}$ relationship per water stress level which is indicated by the Ψ_{leaf}-intercept, Fig. 4) during soil

drying. Overall, plants exhibited different K_{sp} in well-watered conditions and subsequently showed differences in the decrease in K_{sp} during soil drying (Fig. 4). The order of soils in their drop of K_{sp} with soil drying coincides with their order in the *NTR* response to declining Ψ_{soil} (Fig. 3) and the order of their soil hydraulic conductivity curves (Fig. 1B and D), with *NTR* as well as K_{sp} decreasing at higher Ψ_{soil} (see above) and/ or at a considerably higher rate in coarser textured soils during soil drying.

Specifically, in experiment 1, K_{sp} in well-watered conditions was highest in sandy loam, followed by sand (exp. 1, Table 1). In sand (exp. 1), plants have experienced a more severe drop in K_{sp} at relatively less negative Ψ_{leaf} than in sandy loam (Fig. 4A). In the

Fig. 4 Relation between transpiration (*E*) and leaf water potential (Ψ_{leaf}) at different soil water potentials (as indicated by the Ψ_{leaf}-intercept of lines/ circles), comparing mean values of measurements (circles) and the simulation outcomes of the soil-plant hydraulic model (solid lines with confidence inter-
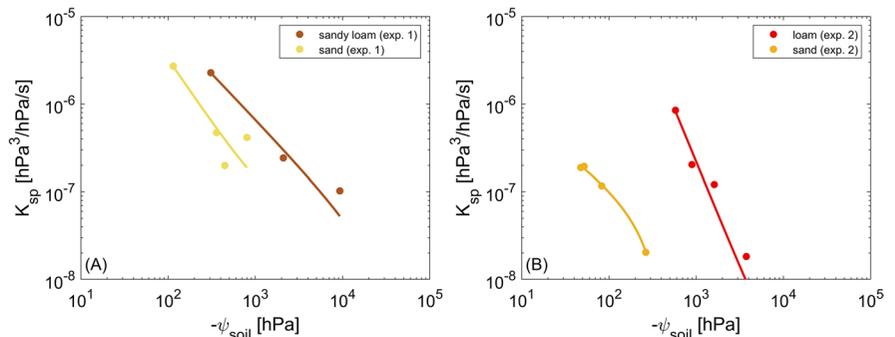
vals, equivalent to soil-plant hydraulic conductance $K_{sp}=\frac{E}{\Delta\Psi_{leaf}}$) during soil drying between different soil textures for: **(A)** exp. 1 sandy loam and sand, and for **(B)** exp. 2 loam and sand. Note that the ranges of *E* between A and B are different as a result of differences in growth conditions

Table 1 Values of soil-plant hydraulic conductance (K_{sp}) in well-watered conditions, active root length (L) and normalized residual mean standard error (NRMSE) for the different soil textures (sandy loam, sand, exp. 2 loam, exp. 2 sand)
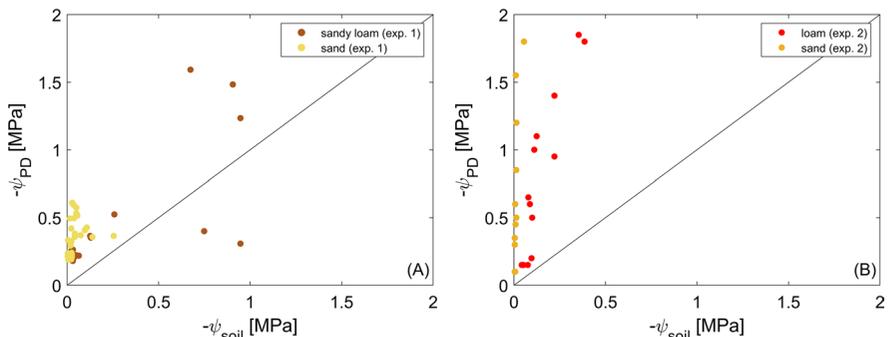
	K_{sp} [cm^3/hPa/s]	L [cm]	NRMSE
sandy loam	2.28×10^{-6}	3630.4	0.1358
sand	1.00×10^{-6}	197.9	0.0531
exp. 2 loam	8.50×10^{-7}	2858.3	0.0366
exp. 2 sand	1.88×10^{-7}	3.2	0.0124

soils used in experiment 2, the soil-plant system was 4.5 times more conductive in loam than in sand (exp. 2) in well-watered conditions (Table 1). While the conductance decreased rapidly with decreasing Ψ_{leaf} in sand (exp. 2), it happened more gradually in loam (Fig. 4B). As K_{sp} was experimentally determined at just two leaf water potentials, the turning point from a linear- to a nonlinear progression of K_{sp} could not be captured. Therefore, the model predictions do not match the measurements perfectly (NRMSE in Table 1). However, the predictions of highest and lowest Ψ_{soil} (as indicated by Ψ_{leaf} at zero transpiration, Fig. 4) in different soil textures were captured well by the model.

Looking at the relationship between experimentally determined soil-plant hydraulic conductivity and Ψ_{soil} at which it got measured, it becomes obvious that in both of the experimental sets, K_{sp} decreased at higher Ψ_{soil} and more steeply in sand, compared to sandy loam (in experiment 1, Fig. 5A) or loam (in experiment 2, Fig. 5B), respectively. Moreover, those curves resemble the soil hydraulic conductivity curves in their relation to each other (Fig. 1B and D).

The pre-dawn leaf water potential (Ψ_{PD}) did not match the soil matric potential (Ψ_{soil}) as calculated from the measured soil water content (Fig. 6). While the measurements scatter around the 1:1 line for sandy loam, they deviate largely from it for the sand (exp. 1) as well as for the in experiment 2 tested loam and sand (exp. 2, Fig. 6A and B). Pre-dawn leaf water potential showed more negative values than the calculated soil matric potential. We will come back to that deviation in the discussion.

Figure 7 shows the relation between daytime leaf water potential and daytime transpiration rate as obtained from the measurements and the model. The resulting curves for the individual soil textures represent the stress onset limit (SOL). The model assumes that transpiration is downregulated at the

Fig. 5 Relationship between experimentally determined soil-plant hydraulic conductance (K_{sp}) and soil water potential (Ψ_{soil}) as measured (dots) and empirically fitted (solid line) during soil drying between different soil textures for: **(A)** exp. 1 sandy loam and sand, and for **(B)** exp. 2 loam and sand
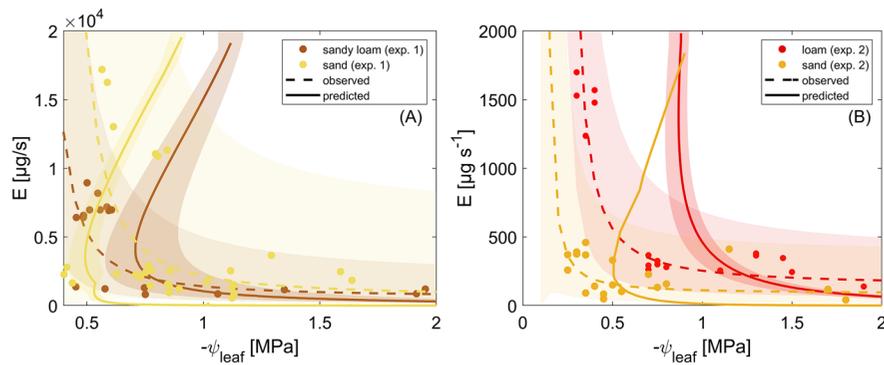

Fig. 6 Relationship between pre-dawn leaf water potential (Ψ_{PD}) and soil water potential (Ψ_{soil}) for: **(A)** exp. 1 sandy loam and sand, and for **(B)** exp. 2 loam and sand

Fig. 7 Relationship between transpiration (*E*) and leaf water potential (Ψ_{leaf}) at the onset of hydraulic limitation (SOL) in response to soil drying between different soils as measured for all replicates (dots), the empirical fit of the observations (dashed line with confidence intervals) and as predcited by the soil-plant hydrauic model (solid line with confidence intervals) for: **(A)** exp. 1 sandy loam and sand, and for **(B)** exp. 2 loam and sand. Note that the ranges of *E* between A and B are different as a result of differences in growth conditions

onset of hydraulic limitation, which is defined as a 30% decrease of K_{sp} from its maximum at a certain soil water potential. Beyond the SOL, a minor increase in transpiration leads to a disproportionally large drop in leaf water potential. Therefore, it has been proposed (Carminati and Javaux 2020) and shown (Abdalla et al. 2021) that stomata promptly close around the SOL (Abdalla et al. 2022). Hence, the SOL can be seen as an indicator for stomatal closure and transpiration reduction. Note that the model predicts an upper boundary of transpiration, rather than an absolute value (Carminati and Javaux 2020). Predicted downregulation of transpiration (and hence, stomata closure) differs visibly between soil textures with plants decreasing their transpiration at the highest leaf water potentials (Ψ_{leaf}) in sand (exp. 1), followed by sandy loam (Fig. 7A, solid lines) in experiment 1, and at higher leaf water potentials in sand (exp. 2) than in loam (Fig. 7B, solid lines) in experiment 2. Hereby, the decline of transpiration is scaled in the same order like the soil hydraulic conductivity curves (Fig. 1B and D). However, the predictions of the onset of hydraulic limitation have to be taken with caution as they do not match the measurements consistently. The measurements are scattered and show no obvious unique relationship between transpiration rate and leaf water potential in dependence of soil hydraulic properties comparing sandy loam and sand (exp. 1) in experiment 1 (Fig. 7A, dashed line and confidence intervals). The difference between soil textures is more pronounced for the soils tested in experiment 2. Plants in sand substrate closed their stomata at less negative leaf water potential (Fig. 7B, dashed line). Potential reasons for those mismatches are discussed in the next section.

The sensitivity analysis showed that *L* did not vary with varying R_p ($=1/K_{sp}$ in well-watered conditions, Supplementary Fig. 3), indicating the uniqueness of the solution and the insensitivity of the model output towards uncertainties in estimating K_p ($= K_{sp}$ in well-watered conditions) from the measurements.

Discussion

For determining the effect of belowground hydraulics on soil-plant water relations during soil drying, we investigated whether and how the responsiveness of maize varied between plants that have been grown in four hydraulically differing soil textures. We combined soil drying experiments with a soil-plant hydraulic model to investigate how those variations are reflected in relationships that consider the plant perspective ($E - \Psi_{leaf}$) as well as the soil perspective ($E - \Psi_{soil}$). We have found that: (i) differences in plant response to soil drying between soil textures became obvious in all displayed relationships, (ii) the predictions as suggested by the model match the experimental results very well from the soil point of view (Figs. 2 and 3), but they (iii) were not entirely consistent in combination with the experimental data from the plant's perspective (Figs. 4 and 7). In

the following, we discuss the effect of soil texture, as belowground hydraulics impacting factor, on plant response to drought.

Transpiration behavior in dependence of declining soil water content as compared between soil textures

In maize, plants grown in different soil textures decreased *NTR* differently with declining soil water content (θ). The critical soil moisture level at which plants started decreasing *NTR* depends on soil textures. Transpiration decreased at lowest water contents in sand (exp. 1) followed by sandy loam (Fig. 2A) and then followed by loam (Fig. 2B). This result is not surprising and it reflects the shape of the water retention curve (Fig. 1A and C, Crawford et al. 1995; Duursma et al. 2008; Hacke et al. 2000).

Transpiration behavior in dependence of declining soil water potential as compared between soil textures

As for the relationship between *NTR* and Ψ_{soil}, maize plants grown in different soil textures responded considerably differently to soil drying (Fig. 3). This result was surprising as this relationship is less commonly implied in models of transpiration response to soil drying (e.g. Agricultural Production Systems Simulator (APSIM, Hammer 1998; Wang et al. 2003), Crop Modeling with Simple Simulation Models (SSM, Soltani and Sinclair 2012), Decision Support System for Agrotechnology Transfer (DSSAT, Jones et al. 2011)). However, earlier evidences of the dependence of the relationship between *NTR* and Ψ_{soil} were reported by Gardner and Ehlig 1963.

The variations in *NTR* - Ψ_{soil} (Fig. 3) between plants grown in these contrasting soil textures correspond well with their unsaturated hydraulic conductivities (Fig. 1B and D), with *NTR* as well as K_s decreasing at less negative Ψ_{soil} and/ or at a less steep rate in sand in both experiments. Despite the differences between the soil hydraulic conductivity in experiment 1 (Fig. 1B) not appearing to be considerable, soil specific features, like soil cracking and crust formation in sandy loam (Supplementary Fig. 4B) are likely to have increased those differences. They are also expected to have encouraged differential root growth- (as indicated by differences in root biomass in experiment 1, Supplementary Table 3) and hence root hydraulic conductivity development (e.g.

decrease in root hydraulic conductivity due to a loss of soil-root contact, Duddek et al. 2022). For example, soil cracking was shown to cause restricted root development and thereby accentuated drought stress (Bandyopadhyay et al. 2003). Moreover, the development of cracks or soil shrinking, might have led roots in close proximity to those cracks to lose contact with the soil (Helliwell et al. 2019). In order to avoid the natural process of the development of soil structure with time in such experimental settings, it would be advisable to let the soil to be tested undergo a succession of wetting and drying to stabilize the soil structure and the soil hydraulic properties in future experiments.

Additionally, the measurements were well reproduced by the soil-plant hydraulic model. Those two findings support one of the major model implications: the importance of the decline in soil hydraulic conductivity and the associated drop in water potential around roots during soil drying (Carminati and Javaux 2020), as soil hydraulic conductivity determines soil-root resistance to water flow and root water uptake as well as transpiration, eventually (Abdalla et al. 2021, 2022).

Variation in soil-plant hydraulic conductance (K_{sp}) during soil drying with contrasting soil textures

Plants grown in different soil textures showed different K_{sp} in wet conditions and a differently rapid decrease in K_{sp} with decreasing Ψ_{soil} (= Ψ_{leaf}-intercept, Fig. 4). In general, the element with the lowest conductance within the SPAC has the strongest influence on the total conductance. At soil water potentials (Ψ_{soil}) of -1 MPa, the soil is expected to become the limiting factor for the total conductance (Draye et al. 2010).

In wet soil conditions, it is well accepted that differences in K_{sp} allude to differences in K_p as affected by different growth media (Maurel and Nacry 2020). The soil plant hydraulic conductivity (K_{sp}) was well fitted by the model in well-watered conditions (Fig. 4, Table 1) and showed soil-specific differences between the plant hydraulic resistance (R_p) and the active root length (L), which emphasizes the effects that soil hydraulic properties have on plant growth and plant- and root hydraulic conductivity development (Lynch 2019; Parent et al. 2009). Note that L is an output of the model and therefore represents only a fraction of the total root length. Hence, it should rather be

taken as a fitting parameter that encompasses several rhizosphere processes that impact the development of water potential gradients around the roots during soil drying. This value will be impacted by the model assumptions, e.g. by assuming water uptake and Ψ_{soil} along the roots to be uniform, or by the assumption that the rhizosphere soil is similar to the bulk soil in its hydraulic properties. However, in maize it was shown that not all roots are equally active in water uptake (Ahmed et al. 2016; Ahmed et al. 2018b). In fact, it has been shown that late metaxylem vessels remain immature and non-conducting 20 or 30 cm from the root tip (McCully and Canny 1988). This adds to the explanation of the small values of L (Table 1).

In contrast, in dry conditions, differences in K_{sp} emphasize the role of soil hydraulic conductivity in limiting the total hydraulic conductance. This is supported by the measured soil-plant hydraulic conductance being scaled with the soil hydraulic conductivity (K_s) of the different soil textures in the dry range (Figs. 1B, D and 5), and by the model having been able to fit the measurements at lowest Ψ_{soil} sufficiently (Fig. 4).

Suitability of using pre-dawn leaf water potential as a predictor of soil water potential

There is a considerable offset between Ψ_{soil} (as determined from soil water content) and Ψ_{PD}, with the calculated Ψ_{soil} being less negative than the measured Ψ_{PD} (Fig. 6). A deviation between soil matric potential and pre-dawn leaf water potential was reported in earlier studies (Abdalla et al. 2021; Cai et al. 2020; Carminati et al. 2017).

On the one hand, Ψ_{PD} might overestimate (in absolute terms) the actual soil matric potential. One reason could be that the night-time transpiration is not exactly zero in maize (Tamang and Sadok 2018 (in our case: 4-15%)), which might have induced fluxes and therefore a more negative Ψ_{PD}. Moreover, Ψ_{PD} is difficult to determine by the Scholander Bomb in well-watered conditions because of a low resolution below 1 bar. Additionally, Ψ_{PD} (absolutely) overestimating Ψ_{soil} hints towards the osmotic potential in the soil potentially having been more negative than in the xylem (in contrast to Abdalla et al. 2022; Cai et al. 2020). In that case, the suction in the xylem would be higher than expected based on the soil matric potential. This is supported by the offset being even bigger in sand (exp. 2) than in loam in experiment 2 (Supplementary Fig. 5B). More nutrients were added to the sand in both experiments and, nutrients are also generally more available in the soil solution in sand. Therefore, the sand (exp. 1 and exp. 2) is likely to have had the highest osmotic potential. On the other hand, Ψ_{soil} as calculated from θ seems to underestimate the actual Ψ_{soil} (in absolute terms). This became especially pronounced in soils that exhibit a steeper soil water retention curve (e.g. exp. 2 sand, Supplementary Fig. 5A). The underestimation of Ψ_{soil} as calculated from θ can be related to a limited possible precision of the TDR measurements (accuracy of the used TDR $= \pm 2\%$), leading to unncertainties in the determination of θ. Moreover, the soil water retention – and conductivity curves as derived from unplanted soil in the laboratory might differ from the actual soil hydraulic properties in the presence of roots in a pot. That said, in future studies, direct measurements of Ψ_{soil} are essential to improve the model performance.

Transpiration response to decreasing leaf water potential under soil drying as compared between soil textures (E - Ψ_{leaf})

The onset of hydraulic limitations in the E - Ψ_{leaf} relationship serves as an indicator for the upper limit of stomatal closure (Carminati and Javaux 2020). The predictions suggest that the same plants, grown in different soils, close stomata and thereby decrease transpiration at different leaf water potentials (Fig. 7). This points towards stomata reacting flexibly to different soil hydraulic properties and supports our hypothesis that there is a link between stomata and belowground hydraulics (Abdalla et al. 2021). These results are in line with the recent finding in tomato with contrasting root system (Abdalla et al. 2022).

However, the model outcomes should be taken with caution, given the comparison with the experimentally determined data. Theoretically, before the soil dependent line of stomata closure, all leaf water potential-transpiration combinations are possible but plants should not cross the line (Fig. 7) as the model predicts an upper boundary to transpiration (Carminati and Javaux 2020). The simulation of the onset of stomata closure is well reflected in the actual measurements in some soils (e.g. exp. 1 sandy loam and

exp. 2 loam) and less well in others (e.g. exp. 1 sand and exp. 2 sand). There are multiple potential reasons for that.

The deviations between model simulations and measurements might stem from the uncertainties that are involved in: (i) the indirect determination of soil water potential (and therefore K_s) from soil water content due to the nonlinear nature of their relationship, and (ii) in the determination of the stress onset limit from measuring Ψ_{leaf} at just two E per soil moisture level. This stresses the importance of measuring Ψ_{soil} directly by installing sensors in the soil rather than to inversely obtain them from soil water content measurements, and Ψ_{leaf} at more than two VPD levels in order to more safely predict the relationship between transpiration and leaf water potential for each water stress level. Lastly, the mismatches between predictions and observations in Fig. 7 might be related to (iii) the applied soil-plant hydraulic model solely capturing the impact of hydraulic processes on transpiration response to soil drying. However, active mechanisms are also known to impact stomatal closure and transpiration reduction (e.g. hormonal signalling, Brodribb and McAdam 2017; Buckley 2019). Therefore, including a stomatal model into the soil plant hydraulic model might improve the predictions of the E - Ψ_{leaf} relationship (e.g. Wankmüller and Carminati 2022).

However, no obvious unique relationship between transpiration and leaf water potential in dependence of soil hydraulic properties in the experimental data might (Fig. 7, dashed lines and confidence intervals of the observations) suggest that plants can react flexibly to changes in soil- and plant water potential by altering the hydraulic conductivity of the rhizosphere. Multiple examples could be proposed for that: xero-branching (Orman-Ligeza et al. 2018), hydrotropism (Dietrich et al. 2017), hydropatterning (Bao et al. 2014), root length (Abdalla et al. 2022), root hairs (Carminati et al. 2017), exudation of mucilage (Ahmed et al. 2014), aquaporin expressions (Chaumont and Tyerman 2014), association with arbuscular mycorrhizal fungi (Abdalla and Ahmed 2021) or plant growth adaptation like circadian oscillations (Caldeira et al. 2014) of root hydraulic conductance (Tardieu et al. 2017). The applied model does not account for such dynamic properties at the soil-root interface which might be a reason for the mismatch between measurements and model predictions.

Taken together, investigating stomata response to drought in soils exhibiting different hydraulic properties clearly hinted towards stomata reacting to changes in belowground hydraulic conductivity.

Conclusion

In conclusion, the soil-plant hydraulic model emphasizes the power of soil hydraulic conductivity and root distribution and -properties for predicting and interpreting transpiration reduction under edaphic drought. The data, in most of the cases, were well reproduced by the model, which supports the link between a soil-specific loss of belowground hydraulic conductivity and stomata regulation.

We identified K_{sp} as a key hydraulic parameter that is central to understand plant adaptation to varying atmospheric and edaphic conditions. It should be measured in more than two VPD levels in order to successfully predict plant response to soil drying.

Moreover, getting the soil water potential and soil hydraulic conductivity right is crucial but not trivial, considering the nonlinear nature of that relationship with soil drying. Indeed, soil moisture has typically been normalized by its maximum (at potting moisture holding capacity) and minimum value (at the wilting point) for comparing crop performances in response to drought, and for evaluating related plant traits, independently from soil texture (e.g. Sinclair 2005). However, our experimental results emphasize the effect of belowground hydraulics on transpiration behavior with soil drying. Therefore, this normalization potentially hides the adaptation and response of plants to different edaphic environments, including root hydraulics related traits. Hence, it might be worth to consider investigating belowground traits in the context of phenotyping experiments (Atkinson et al. 2014; Cai et al. 2022).

An additional complexity is introduced by a drop in the hydraulic conductivity at the soil-root interface as a consequence of roots and root hairs losing contact with the soil due to shrinking with soil drying (Duddek et al. 2022). Therefore, including the dynamic properties of the root–soil interface appears important to properly understand belowground limitations. We conclude, that predictions of transpiration response to drought need to consider soil-root hydraulics as well as plant traits, as roots and the soil-root-interface

are key hydraulic regions that plants can alter to efficiently adapt to water limitations.

Author contributions MAA and JK acquired the funding. TK, AB, DSB, SK, TM, AC, JK and MAA designed the concept of this study. TK, AB, DSB, SK and TM conducted the field work and sampled the data with help and input from AC, JK and MAA. DB and GPB measured ABA concentrations and analysed data. TK analysed the data. MZ assisted with the simulations. TK wrote the manuscript with contributions from AC, JK, DB and MAA.

Data availability The datasets generated during and/or analysed during the current study are available from the corresponding author on reasonable request.

Declarations

Competing interests The authors declare that the research was conducted in the absence of any commercial or financial relationships that could be construed as a potential conflict of interest.

References

Abdalla M, Ahmed MA (2021) Arbuscular mycorrhiza Symbiosis enhances water status and soil-plant hydraulic conductance under drought. Front Plant Sci 12:722954. https://doi.org/10.3389/fpls.2021.722954

Abdalla M, Carminati A, Cai G, Javaux M, Ahmed MA (2021) Stomatal closure of tomato under drought is driven by an increase in soil-root hydraulic resistance. Plant Cell Environ 44(2):425–431. https://doi.org/10.1111/pce.13939

Abdalla M, Ahmed MA, Cai G, Wankmüller F, Schwartz N, Litig O, Javaux M, Carminati A (2022) Stomatal closure during water deficit is controlled by belowground hydraulics. Ann Bot 129(2):161–170. https://doi.org/10.1093/aob/mcab141

Ahmed MA, Kroener E, Holz M, Zarebanadkouki M, Carminati A (2014) Mucilage exudation facilitates root water uptake in dry soils. Funct Plant Biol 41(11):1129–1137. https://doi.org/10.1071/FP13330

Ahmed MA, Zarebanadkouki M, Kaestner A, Carminati A (2016) Measurements of water uptake of maize roots: the key function of lateral roots. Plant Soil 398(1-2):59–77. https://doi.org/10.1007/s11104-015-2639-6

Ahmed MA, Passioura J, Carminati A (2018a) Hydraulic processes in roots and the rhizosphere pertinent to increasing yield of water-limited grain crops: a critical review. J Exp Bot 69(13):3255–3265. https://doi.org/10.1093/jxb/ery183

Ahmed MA, Zarebanadkouki M, Meunier F, Javaux M, Kaestner A, Carminati A (2018b) Root type matters: measurement of water uptake by seminal, crown, and lateral roots in maize. J Exp Bot 69(5):1199–1206. https://doi.org/10.1093/jxb/erx439

Anderegg WRL, Wolf A, Arango-Velez A, Choat B, Chmura DJ, Jansen S, Kolb T, Li S, Meinzer F, Pita P, Resco de Dios V, Sperry JS, Wolfe BT, Pacala S (2017) Plant water potential improves prediction of empirical stomatal models. PLoS One 12(10):e0185481. https://doi.org/10.1371/journal.pone.0185481

Atkinson JA, Rasmussen A, Traini R, Voß U, Sturrock C, Mooney SJ, Wells DM, Bennett MJ (2014) Branching out in roots: uncovering form, function, and regulation. Plant Physiol 166(2):538–550. https://doi.org/10.1104/pp.114.245423

Bandyopadhyay KK, Mohanty M, Painuli DK, Misra AK, Hati KM, Mandal KG, Ghosh PK, Chaudhary RS, Acharya CL (2003) Influence of tillage practices and nutrient management on crack parameters in a vertisol of Central India. Soil Tillage Res 71(2):133–142. https://doi.org/10.1016/S0167-1987(03)00043-6

Bao Y, Aggarwal P, Robbins NE, Sturrock CJ, Thompson MC, Tan HQ, Tham C, Duan L, Rodriguez PL, Vernoux T, Mooney SJ, Bennett MJ, Dinneny JR (2014) Plant roots use a patterning mechanism to position lateral root branches toward available water. Proc Natl Acad Sci 111(25):9319–9324. https://doi.org/10.1073/pnas.1400966111

Barnston AG (1992) Correspondence among the correlation, RMSE, and Heidke forecast verification measures; refinement of the Heidke score. Weather Forecast 7(4):699–709. https://doi.org/10.1175/1520-0434(1992)007<0699:CATCRA>2.0.CO;2

Brodribb TJ, McAdam SAM (2017) Evolution of the stomatal regulation of plant water content. Plant Physiol 174(2):639–649. https://doi.org/10.1104/pp.17.00078

Brodribb TJ, Sussmilch F, McAdam SAM (2019) From reproduction to production, stomata are the master regulators. Plant J 101(4):756–767. https://doi.org/10.1111/tpj.14561

Buckley TN (2019) How do stomata respond to water status? New Phytol 224(1):21–36. https://doi.org/10.1111/nph.15899

Cai G, Ahmed MA, Dippold MA, Zarebanadkouki M, Carminati A (2020) Linear relation between leaf xylem water potential and transpiration in pearl millet during soil drying. Plant Soil 447(1-2):565–578. https://doi.org/10.1007/s11104-019-04408-z

Cai G, Carminati A, Abdalla M, Ahmed MA (2021) Soil textures rather than root hairs dominate water uptake and soil-plant hydraulics under drought. Plant Physiol 187(2):858–872. https://doi.org/10.1093/plphys/kiab271

Cai G, Ahmed MA, Abdalla M, Carminati A (2022) Root hydraulic phenotypes impacting water uptake in drying soils. Plant Cell Environ 45(3):650–663. https://doi.org/10.1111/pce.14259

Caldeira CF, Jeanguenin L, Chaumont F, Tardieu F (2014) Circadian rhythms of hydraulic conductance and growth are enhanced by drought and improve plant performance. Nat Commun 5(1):5365. https://doi.org/10.1038/ncomms6365

Carminati A, Javaux M (2020) Soil rather than xylem vulnerability controls stomatal response to drought. Trends Plant Sci 25(9):868–880. https://doi.org/10.1016/j.tplants.2020.04.003

Carminati A, Passioura JB, Zarebanadkouki M, Ahmed MA, Ryan PR, Watt M, Delhaize E (2017) Root hairs enable high transpiration rates in drying soils. New Phytol 216(3):771–781. https://doi.org/10.1111/nph.14715

Chaumont F, Tyerman SD (2014) Aquaporins: highly regulated channels controlling plant water relations. Plant Physiol 164(4):1600–1618. https://doi.org/10.1104/pp.113.233791

Crawford JW, Matsui N, Young IM (1995) The relation between the moisture-release curve and the structure of soil. Eur J Soil Sci 46(3):369–375. https://doi.org/10.1111/j.1365-2389.1995.tb01333.x

Devi JM, Sinclair TR, Vadez V (2010) Genotypic variability among peanut (Arachis hypogea L.) in sensitivity of nitrogen fixation to soil drying. Plant Soil 330(1-2):139–148. https://doi.org/10.1007/s11104-009-0185-9

Dietrich D, Pang L, Kobayashi A, Fozard JA, Boudolf V, Bhosale R, Antoni R, Nguyen T, Hiratsuka S, Fujii N, Miyazawa Y, Bae T-W, Wells DM, Owen MR, Band LR, Dyson RJ, Jensen OE, King JR, Tracy SR et al (2017) Root hydrotropism is controlled via a cortex-specific growth mechanism. Nature Plants 3(6):17057. https://doi.org/10.1038/nplants.2017.57

Draye X, Kim Y, Lobet G, Javaux M (2010) Model-assisted integration of physiological and environmental constraints affecting the dynamic and spatial patterns of root water uptake from soils. J Exp Bot 61(8):2145–2155. https://doi.org/10.1093/jxb/erq077

Duddek P, Carminati A, Koebernick N, Ohmann L, Lovric G, Delzon S, Rodriguez-Dominguez CM, King A, Ahmed MA (2022) The impact of drought-induced root and root hair shrinkage on root-soil contact. Plant Physiol 189(3):1232–1236. https://doi.org/10.1093/plphys/kiac144

Durner W (1994) Hydraulic conductivity estimation for soils with heterogeneous pore structure. Water Resour Res 30(2):211–223. https://doi.org/10.1029/93WR02676

Duursma RA, Kolari P, Perämäki M, Nikinmaa E, Hari P, Delzon S, Loustau D, Ilvesniemi H, Pumpanen J, Mäkelä A (2008) Predicting the decline in daily maximum transpiration rate of two pine stands during drought based on constant minimum leaf water potential and plant hydraulic conductance. Tree Physiol 28(2):265–276. https://doi.org/10.1093/treephys/28.2.265

Gahoonia TS, Nielsen NE (2003) Phosphorus (P) uptake and growth of a root hairless barley mutant (bald root barley, brb) and wild type in low- and high-P soils. Plant Cell Environ 26(10):1759–1766. https://doi.org/10.1046/j.1365-3040.2003.01093.x

Gardner WR (1960) Dynamic aspects of soil-water availability to plants. Annu Rev Plant Physiol 16(1):323–342

Gardner WR, Ehlig CF (1963) The influence of soil water on transpiration by plants. J Geophys Res 68(20):5719–5724. https://doi.org/10.1029/JZ068i020p05719

Hacke UG, Sperry JS, Ewers BE, Ellsworth DS, Schäfer KVR, Oren R (2000) Influence of soil porosity on water use in Pinus taeda. Oecologia 124(4):495–505. https://doi.org/10.1007/pl00008875

Hammer GL (1998) Crop modelling: current status and opportunities to advance. Acta Horticulturae (456): 27–36. https://doi.org/10.17660/actahortic.1998.456.1

Hayat F, Ahmed MA, Zarebanadkouki M, Javaux M, Cai G, Carminati A (2020) Transpiration reduction in maize (Zea mays L) in response to soil drying. Front Plant Sci 10(1):1695. https://doi.org/10.3389/fpls.2019.01695

Helliwell JR, Sturrock CJ, Miller AJ, Whalley WR, Mooney SJ (2019) The role of plant species and soil condition in the structural development of the rhizosphere. Plant Cell Environ 42(6):1974–1986. https://doi.org/10.1111/pce.13529

Hopmans and Bristow (2002) Current capabilities and future needs of root water and nutrient uptake modeling. Advances in agronomy. Academic Press, Cambridge, p 77

Jasechko S, Sharp ZD, Gibson JJ, Birks SJ, Yi Y, Fawcett PJ (2013) Terrestrial water fluxes dominated by transpiration. Nature 496(7445):347–350. https://doi.org/10.1038/nature11983

Jones et al (2011) Decision support system for agrotechnology transfer: DSSAT v3. Understanding options for agricultural production. Springer, Berlin, p 7

Kholová J, Hash CT, Kakkera A, Kocová M, Vadez V (2010) Constitutive water-conserving mechanisms are correlated with the terminal drought tolerance of pearl millet Pennisetum glaucum (L.) R. Br. J Exp Bot 61(2):369–377. https://doi.org/10.1093/jxb/erp314

Lynch JP (2019) Root phenotypes for improved nutrient capture: an underexploited opportunity for global agriculture. New Phytol 223(2):548–564. https://doi.org/10.1111/nph.15738

Maurel C, Nacry P (2020) Root architecture and hydraulics converge for acclimation to changing water availability. Nature Plants 6(7):744–749. https://doi.org/10.1038/s41477-020-0684-5

McCully ME, Canny MJ (1988) Pathways and processes of water and nutrient movement in roots. Plant Soil 111(2):159–170. https://doi.org/10.1007/BF02139932

Orman-Ligeza B, Morris EC, Parizot B, Lavigne T, Babb A, Ligeza A, Klein S, Sturrock C, Xuan W, Novvk O, Ljung K, Rodriguez PL, Fernandez M, Dodd IC, de Smet I, Chaumont F, Batoko H, PPrilleux C, Lynch JP et al (2018) The Xerobranching response represses lateral root formation when roots are not in contact with water. Curr Biol 28(19):3165–3173. https://doi.org/10.2139/ssrn.3188447

Parent B, Hachez C, Redondo E, Simonneau T, Chaumont F, Tardieu F (2009) Drought and abscisic acid effects on aquaporin content translate into changes in hydraulic conductivity and leaf growth rate: a trans-scale approach. Plant Physiol 149(4):2000–2012. https://doi.org/10.1104/pp.108.130682

Passioura J (1980) The transport of water from soil to shoot in wheat seedlings. J Exp Bot 31(1):333–345. https://doi.org/10.1093/jxb/31.1.333

Pathak P, Sudi R, Wani SP, Sahrawat KL (2013) Hydrological behavior of Alfisols and Vertisols in the semi-arid zone: implications for soil and water management. Agric Water Manag 118:12–21. https://doi.org/10.1016/j.agwat.2012.11.012

Ritchie and Hinckley (1975) The Pressure Chamber as an Instrument for Ecological Research. Advances in Ecological Research. 9. Academic Press, Cambridge

Rodrigues O, Reshetnyak G, Grondin A, Saijo Y, Leonhardt N, Maurel C, Verdoucq L (2017) Aquaporins facilitate hydrogen peroxide entry into guard cells to mediate ABA- and pathogen-triggered stomatal closure. Proc Natl Acad Sci 114(34):9200–9205. https://doi.org/10.1073/pnas.1704754114

Rodriguez-Dominguez CM, Brodribb TJ (2020) Declining root water transport drives stomatal closure in olive under moderate water stress. New Phytol 225(1):126–134. https://doi.org/10.1111/nph.16177

Sinclair TR (2005) Theoretical analysis of soil and plant traits influencing daily plant water flux on drying soils. Agron J 97(4):1148–1152. https://doi.org/10.2134/agronj2004.0286

Soltani and Sinclair (2012) Modeling physiology of crop development, growth and yield. CABI Publication, Wallingford

Tamang BG, Sadok W (2018) Nightly business: links between daytime canopy conductance, nocturnal transpiration and its circadian control illuminate physiological trade-offs in maize. Environ Exp Bot 148(1):192–202. https://doi.org/10.1016/j.envexpbot.2017.11.016

Tardieu F, Draye X, Javaux M (2017) Root water uptake and Ideotypes of the root system: whole-plant controls matter. Vadose Zone J 16(9):1–10. https://doi.org/10.2136/vzj2017.05.0107

Tardieu F, Simonneau T, Muller B (2018) The physiological basis of drought tolerance in crop plants: a scenario-dependent probabilistic approach. Annu Rev Plant Biol 69(1):733–759. https://doi.org/10.1146/annurev-arplant-042817-040218

Vetterlein D, Lippold E, Schreiter S, Phalempin M, Fahrenkampf T, Hochholdinger F, Marcon C, Tarkka M, Oburger E, Ahmed M, Javaux M, Schlüter S (2021) Experimental platforms for the investigation of spatiotemporal patterns in the rhizosphere—laboratory and field scale. J Plant Nutr Soil Sci 184(1):35–50. https://doi.org/10.1002/jpln.202000079

Wang E, Robertson MR, Hammer GL, Carberry P, Holzworth D, Hargreaves J, Huth N, Chapman S, Meinke H, McLean G (2003) Design and implementation of a generic crop module template in the cropping system model APSIM. Eur J Agronomy 18(1-2):121–140

Wankmüller FJP, Carminati A (2022) Stomatal regulation prevents plants from critical water potentials during drought: result of a model linking soil–plant hydraulics to abscisic acid dynamics. Ecohydrology 15(5). https://doi.org/10.1002/eco.2386